JCTC Journal of Chemical Theory and Computation

Article

pubs.acs.org/JCTC

Molecular Excitation Energies from Time-Dependent Density Functional Theory Employing Random-Phase Approximation Hessians with Exact Exchange

Andreas Heßelmann*

Lehrstuhl für Theoretische Chemie, Universität Erlangen-Nürnberg, Egerlandstr. 3, D-91058 Erlangen, Germany

ABSTRACT: Molecular excitation energies have been calculated with time-dependent density-functional theory (TDDFT) using random-phase approximation Hessians augmented with exact exchange contributions in various orders. It has been observed that this approach yields fairly accurate local valence excitations if combined with accurate asymptotically corrected exchange-correlation potentials used in the ground-state Kohn−Sham calculations. The inclusion of long-range particle−particle with hole−hole interactions in the kernel leads to errors of 0.14 eV only for the lowest excitations of a selection of three alkene, three carbonyl, and five azabenzene molecules, thus surpassing the accuracy of a number of common TDDFT and even some wave function correlation methods. In the case of long-range charge-transfer excitations, the method typically underestimates accurate reference excitation energies by 8% on average, which is better than with standard hybrid-GGA functionals but worse compared to range-separated functional approximations.

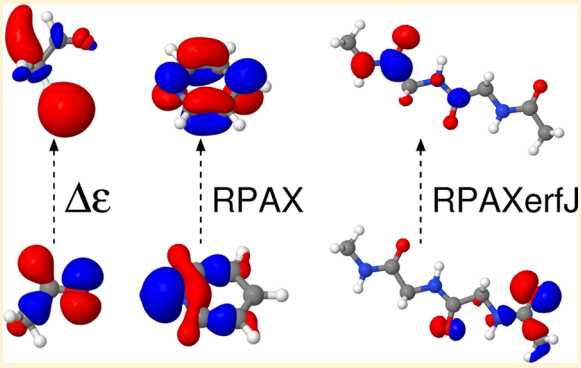

1. INTRODUCTION

Time-dependent density functional theory (TDDFT) methods which are based on the linear-response approach are nowadays the most widely used approaches for studying excited states of medium sized and large molecules.[1−6] Based on the Runge−Gross theorem,[7] which generalizes the Hohenberg−Kohn theorem[8] for ground-state properties to time-dependent properties, TDDFT methods are potentially exact. This means that they enable the calculation of (linear) response properties and excitation energies without any approximation (in the framework of the nonrelativistic and Born−Oppenheimer approximation) if the underlying exact exchange-correlation (xc) potential and kernel were known.

Exact or almost exact xc potentials can be obtained from ab initio molecular densities that are accessible from accurate wave function methods. For this, various methods have been developed with which the Kohn−Sham equations can be inverted, i.e., by which the unknown xc potential v_{xc} can be determined from a given density ρ.[9−18] It has been observed by van Gisbergen et al. that TDDFT methods which employ xc potentials derived from accurate configuration-interaction wave function densities provide very accurate polarizabilities and singlet and triplet excitations for a number of atoms even if combined with approximate xc kernels,[19] namely the adiabatic local density approximation (ALDA) xc kernel. This shows, at least for certain classes of excitations, that already the xc potential has a large impact on the accuracy of the considered excitation. Other classes of excitations, e.g., charge-transfer (CT) excitations or double excitations, cannot be described with local adiabatic approximations to the xc kernel and require more elaborate approximations to the unknown exact xc kernel.[20−29]

In praxis, TDDFT calculations are commonly carried out using (hybrid- or meta-) generalized-gradient approximation (GGA) functionals[30] from which the xc potential and kernel are derived as the first and second functional derivative. Two recent benchmarks by Caricato et al.[31] and Jacquemin et al.[32] have demonstrated that generally hybrid-GGA functionals like PBE0 or B3P86 with 20−30% of exact exchange provide the best accuracy among the tested functionals, even if compared with more recent hybrid-GGA and range-separated functionals. If long-range charge-transfer excitations are considered, however, the latter class of functionals, the range-separated functionals, yield the best accuracy as has been shown in a number of works.[33−37] The reason for this is that, compared to hybrid functionals, in these functionals nonlocal exact-exchange contributions are mixed with a larger percentage with the local exchange functionals in the asymptotic range (for large electron−electron distances). Also some long-range corrections to existing xc kernels have been developed in order to describe CT excitations with TDDFT methods.[23,38]

Since it is known that the accuracy of TDDFT excitation energies of local valence excitations and also of Rydberg-type excitations strongly depend on the quality of the underlying exchange-correlation potential, a number of model xc potentials have been developed in order to improve the deficiencies of standard GGA or hybrid-GGA xc potentials.[12,13,39−47] In

Received: January 12, 2015

DOI: 10.1021/acs.jctc.5b00024
J. Chem. Theory Comput. XXXX, XXX, XXX−XXX

particular, asymptotic correction schemes to standard GGA and hybrid-GGA potentials have been developed for enforcing the correct asymptotic behavior of $-1/r$ of the exact xc potential.[48−54] Numerical results for excitation energies for a range of small molecules using these model xc potentials (combined with standard ALDA or AGGA xc kernels) considerably improve upon (vertical) excitation energies obtained with standard GGA and even hybrid-GGA functionals.[48−50,52] Most remarkably, TDDFT calculations with asymptotically corrected xc potentials are even able to achieve accuracies comparable to more expensive wave function correlation methods like CASPT2[48] or EOM-CCSD.[55]

In this work, the influence of the exchange-correlation kernel on molecular excitation energies will be investigated. For this, an accurate model xc potential for the ground-state KS calculation is combined with Coulomb and xc kernels in various approximations in the TDDFT calculation. In particular, contrary to standard TDDFT methods based on the GGA approach, exact nonlocal exchange effects will be accounted for in different approximations to the xc kernel. The exact nonlocal and nonadiabatic exchange (EXX) kernel has been derived by Görling[20,21] and has numerically been tested by Hirata et al.[55,56] and also in refs 28, 29, 57, and 58. While it has been proven that the EXX kernel resolves the charge-transfer problem which plagues current TDDFT approaches,[28] the results of ref 58 indicate that TDDFT methods using the EXX kernel yield excitation energies which are close to corresponding TDHF results. This means that local valence excitations become worse with this approach if compared to standard TDDFT methods based on local xc kernels. However, other versions of exchange-RPA methods which use different Coulomb+exchange correlation couplings, have been used recently to calculate ground-state correlation energies in the framework of the adiabatic-connection fluctuation−dissipation theorem (AC-FDT).[59−62] While the corresponding AC-FDT method which employs the full exact-exchange kernel, termed EXX-RPA,[63−65] has been shown to yield accurate total energies or reaction energies,[63,65] these other exchange-RPA methods exclude particle−particle+hole−hole interaction contributions to the many-body expansion of the response function.[59−62] Despite the fact that these approaches are less complete than EXX-RPA regarding the number of terms in each order of the many-body expansion of the correlation energy, some of them yield very accurate thermodynamic properties for a range of small molecules.[60−62] The reason why particle−particle+hole−hole Coulomb interaction contributions can be omitted in exchange-RPA methods is analyzed in ref 62.

Because of the promising results of particle-hole exchange-RPA methods for describing ground-state correlation energies, here the effect of particle-hole exchange interactions on excited states will be tested. Missing particle−particle+hole−hole interactions in the exchange kernel, that are known to be crucial for the description of charge-transfer excited states,[28] will be accounted for only for long-range interactions, i.e., only for larger electron−electron distances.

This work is organized as follows: Section 2 describes the derivations of the xc potential (2.1) and xc kernel (2.2, 2.3, and 2.4) used in the calculations; section 2.5 summarizes the methods introduced in the sections 2.1−2.4. Section 3 describes the computational details, and section 4 presents the results for local valence and Rydberg excitations (4.1) and charge-transfer excitations (4.3). Section 5 presents a summary of the results.

2. METHOD

2.1. Exchange-Correlation Potential. The two exchange-correlation (xc) potentials used in this work are two localized and asymptotically corrected variants of the PBE0 (hybrid Perdew−Burke−Ernzerhof functional) xc potential,[66−68] which is defined as

$$v_{\mathrm{xc}}^{\mathrm{PBE0}}(\mathbf{r},\mathbf{r}') = \frac{3}{4}\frac{\delta E_{\mathrm{x}}^{\mathrm{PBE}}}{\delta\rho(\mathbf{r})}\delta(\mathbf{r}-\mathbf{r}') + \frac{1}{4}\frac{-\gamma(\mathbf{r},\mathbf{r}')}{|\mathbf{r}-\mathbf{r}'|} + \frac{\delta E_{\mathrm{c}}^{\mathrm{PBE}}}{\delta\rho(\mathbf{r})}\delta(\mathbf{r}-\mathbf{r}') \tag{1}$$

with $E_{\mathrm{x}}^{\mathrm{PBE}}$ being the PBE exchange-functional,[66] $E_{\mathrm{c}}^{\mathrm{PBE}}$ the PBE correlation functional,[66] and $\rho(\mathbf{r})$ and $\gamma(\mathbf{r},\mathbf{r}')$ are the density and one-particle density matrix, respectively. The second nonlocal contribution to $v_{\mathrm{xc}}^{\mathrm{PBE0}}$ in eq 1 originates from the functional derivative (with respect to the density-matrix) of the exact exchange energy functional and is sometimes also referred to as Hartree−Fock potential $v_{\mathrm{x}}^{\mathrm{NL}}(\mathbf{r},\mathbf{r}')$ (though γ here is evaluated using Kohn−Sham orbitals instead of Hartree−Fock orbitals).

Due to the nonlocality of $v_{\mathrm{xc}}^{\mathrm{PBE0}}$, DFT methods employing the PBE0 functional are no pure Kohn−Sham methods anymore, and orbital energies from such hybrid-DFT methods show significant differences to Kohn−Sham orbital energies, especially for the unoccupied states, see e.g. refs 23 and 69. Since, on the other hand, orbital energy differences of occupied and virtual Kohn−Sham single-particle states can serve as a first approximation to valence excitations of a molecular system,[70] the use of pure Kohn−Sham methods instead of generalized ones can have advantages regarding the characterization of electronic transitions as calculated by TDDFT. Because of this, in this work the nonlocal contribution $v_{\mathrm{x}}^{\mathrm{NL}}(\mathbf{r},\mathbf{r}')$ to $v_{\mathrm{xc}}^{\mathrm{PBE0}}$ is replaced by two local approximations to the nonlocal exact exchange potential, namely the EXX (exact-exchange) potential[71−73] and the Becke−Roussel−Johnson meta-GGA approximation to $v_{\mathrm{x}}^{\mathrm{NL}}(\mathbf{r},\mathbf{r}')$.[46,74]

The EXX potential $v_{\mathrm{x}}^{\mathrm{EXX}}(\mathbf{r})$ is the functional derivative (with respect to the density) of the exact exchange energy functional and can be calculated by solving the OEP (Optimized Effective Potential) integral equation:[71,72,75−78]

$$\int \mathrm{d}\mathbf{r}'\chi_0(\mathbf{r},\mathbf{r}')\, v_{\mathrm{x}}^{\mathrm{EXX}}(\mathbf{r}') = 2\sum_{ia}\phi_i(\mathbf{r})\,\phi_a(\mathbf{r})\,\frac{\langle\phi_i|v_{\mathrm{x}}^{\mathrm{NL}}|\phi_a\rangle}{\varepsilon_i-\varepsilon_a} \tag{2}$$

with χ_0 being the uncoupled Kohn−Sham response function and ϕ_i,ϕ_a and $\varepsilon_i,\varepsilon_a$ denoting the (real-valued) occupied/virtual Kohn−Sham spin−orbitals and orbital energies, respectively.

Compared to this, the Becke−Roussel−Johnson meta-GGA is a local approximation to the nonlocal exact exchange potential and is defined as[46,74,79,80]

$$v_{\mathrm{x}}^{\mathrm{BRJ}}(\mathbf{r}) = -\int \mathrm{d}\mathbf{r}'\,\frac{\rho_{\mathrm{x}}^{\mathrm{BR}}(\mathbf{r},\mathbf{r}')}{|\mathbf{r}-\mathbf{r}'|} + C_{\Delta V}\sqrt{\frac{\tau(\mathbf{r})}{\rho(\mathbf{r})}} \tag{3}$$

where $\rho_{\mathrm{x}}^{\mathrm{BR}}$ is the Becke−Roussel meta-GGA approximation to the exchange-hole,[74,79] τ is the kinetic energy density, and $C_{\Delta V}$ is a constant value which has been defined by the uniform electron gas limit of τ by Becke and Johnson.[46] The first term on the right-hand side in eq 3 can be identified as the Slater potential contribution to v_x, while the second term models the typical step structure of the response potential contribution to

DOI: 10.1021/acs.jctc.5b00024
J. Chem. Theory Comput. XXXX, XXX, XXX−XXX

v_x, see refs 81−83. It has been observed that the local exchange model potential of eq 3 reproduces the exact-exchange potential (from OEP calculations) well if the γ factor in the meta-GGA model of ρ_x, see refs 74 and 80, is set to a value of $\gamma = 1.15$.[80]

Substituting the nonlocal exchange potential in eq 1 by either of the two local exact-exchange potentials $v_x^{EXX/BRJ}$ yields the following localized PBE0 xc potential:

$$v_{xc}^{LPBE0}(\mathbf{r}) = \frac{3}{4}\frac{\delta E_x^{PBE}}{\delta\rho(\mathbf{r})} + \frac{1}{4}v_x^{EXX/BRJ}(\mathbf{r}) + \frac{\delta E_c^{PBE}}{\delta\rho(\mathbf{r})} \tag{4}$$

This xc potential does not exhibit the correct asymptotic behavior of $-1/r$ of the exact xc potential which is crucial in order to obtain a correct description of Rydberg excited states, see section 4.1. This is so, because the GGA part to the local exchange potential vanishes exponentially in the asymptotic range, so that $v_{xc}^{LPBE0}(r) \xrightarrow[r\to\infty]{} -\frac{1}{4}r$. In order to correct this, the shift-and-splice method can be used in which the bulk potential, i.e., the potential in the vicinity around the nuclei, is first shifted by the derivative discontinuity of the molecule and then spliced with an asymptotically correct behaving potential to describe the asymptotic range, see refs 48, 49, 51, and 52. As an alternative, the correct asymptotic behavior can also be obtained by the charge constraint within the OEP method (termed OEP-AC in this work), see 54 and 78. In order to apply this to the LPBE0 xc potential of eq 4, the nonlocal exchange potential v_x^{NL} simply has to be substituted by either the PBE0 (eq 1) or the LPBE0 (eq 4) xc potentials in the OEP eq 2. In addition, the HOMO constraint[78] can be employed in order to enforce the HOMO orbital energy to be identical to the negative ionization energy which corrects the integer-continutity of the GGA contribution to the xc potential.

In this work, both for the LPBE0 potential using the EXX local exact-exchange potential and the LPBE0 potential using the BRJ exchange model potential, the second of the above-noted asymptotic correction schemes was used (in order to distinguish between these two model xc potentials, in the following the asymptotically corrected EXX-based potential will be termed as PBE0AC(EXX) and the BRJ-based potential as PBE0AC(BRJ)). Thereby it was observed that molecular excitation energies calculated with xc potentials obtained by the two asymptotic correction methods showed only marginal differences for valence- and low-lying Rydberg excited states, but for higher lying Rydberg states the OEP-AC method was found to be more accurate due to the fact that xc potential matrix elements involving diffuse functions are calculated analytically in this method while in the shift-and-splice scheme a numerical quadrature is used. This can lead to numerical inaccuracies even with tight standard quadrature grids if the basis functions are very diffuse, because these grids still are too coarse in the asymptotic range. The ionization energies required for the HOMO constraint within the OEP-AC method were obtained by separate PBE0 calculations of the respective neutral and the positively charged molecule.

2.2. Exchange-Correlation Kernel. Excitation energies from a time-dependent DFT (or Hartree−Fock) method which excludes any exchange-correlation (xc) contributions (i.e., functional derivatives of the xc potential) can be obtained from the solution to the (non-Hermitian) random-phase approximation (RPA) eigenvalue equation (the orbitals are, without the restriction of generality, assumed to be real-valued):

$$\left[\begin{pmatrix}\Delta\varepsilon & \mathbf{0}\\ \mathbf{0} & \Delta\varepsilon\end{pmatrix} + \begin{pmatrix}\mathbf{C} & \mathbf{C}\\ \mathbf{C} & \mathbf{C}\end{pmatrix}\right]\begin{pmatrix}\mathbf{X}_p\\ \mathbf{Y}_p\end{pmatrix} = \omega_p\begin{pmatrix}-\mathbf{1} & \mathbf{0}\\ \mathbf{0} & \mathbf{1}\end{pmatrix}\begin{pmatrix}\mathbf{X}_p\\ \mathbf{Y}_p\end{pmatrix} \tag{5}$$

where $\Delta\varepsilon_{ia} = (\varepsilon_a - \varepsilon_i)\delta_{ij}\delta_{ab}$ is a diagonal submatrix containing the orbital energy differences between occupied (labeled *i,j,...*) and virtual (labeled *a,b,...*) orbitals, $\mathbf{C}$ is defined as $C_{ia,jb} = [ia|jb]$ (two-electron integral in chemist's notation) with indices *i,j* and *a,b* combined to superindices *ia* and *jb* (occupied-virtual orbital pair) and the vector $(\mathbf{X}_p\ \mathbf{Y}_p)^T$ denotes the *p*th eigenvector corresponding to the *p*th excitation energy ω_p. The sub-blocks of the Hessian matrix in eq 5 originate from the coupling of the single-excited determinants (Φ_i^a,Φ_j^b) and the coupling of the doubly excited determinants with the ground state (Φ_{ij}^{ab}, Φ_0), more precisely:

$$(\Delta\varepsilon + C)_{ia,jb} = \langle\Phi_i^a|\hat{H} - E_0|\Phi_j^b\rangle^H \tag{6}$$

$$C_{ia,jb} = \langle\Phi_0|\hat{H} - E_0|\Phi_{ij}^{ab}\rangle^H \tag{7}$$

In eqs 6 and 7, the modified $\langle...\rangle^H$ Dirac notation here shall indicate that only direct particle−hole electron−electron interaction terms are accounted for in the contribution to the Hessian matrix.

In order to go beyond the RPA approximation, in addition to the Coulomb interaction contributions in eq 5, exchange and correlation interaction terms have to be accounted for. While exchange interactions still can be described within the single-determinant approximation (ϕ_0) to the ground-state wave function, the inclusion of correlation interaction contributions for describing the excited states would require a multi-determinant ansatz for the ground state. In standard TDDFT methods (i.e., TDDFT methods based on the LDA or GGA approximations), however, correlation (and exchange) effects to the electronic Hessian matrix are described by the second functional derivative (with respect to the density) of a local xc functional. Then the above RPA eqs 6 and 7 for the Hessian can be transformed into the TDDFT Hessian by the substitution

$$C_{ia,jb} \to F_{ia,jb} = C_{ia,jb} + [ia|f_{xc}|jb] \tag{8}$$

where $f_{xc}(\mathbf{r}) = \delta E_{xc}/(\delta\rho(\mathbf{r})\ \delta\rho(\mathbf{r}'))\delta(\mathbf{r} - \mathbf{r}')$ and E_{xc} is the xc energy in the LDA/GGA approximation.

In this work, while too starting from a Kohn−Sham ground-state determinant, see section 2.1, the RPA approximation (eqs 5, 6, and 7) shall be corrected by explicitly including the exchange interaction contributions that are skipped in the eqs 6 and 7. For this, it is assumed that the Kohn−Sham orbitals building the Kohn−Sham determinant can be transformed into Hartree−Fock orbitals by an occupied−occupied and virtual−virtual unitary transformation, i.e., it is assumed that the Kohn−Sham determinant too minimizes the energy expectation value. It has been analyzed in previous works that for the case of the exchange-only KS determinant this is virtually fulfilled[28,29,84] (in fact, the EXX method minimizes the same energy expectation value as the HF method, but under the constraint of a local KS potential[85]). Then the sub-blocks of the Hessian matrix in eqs 6 and 7 take the same form as in the case of the TDHF method:[58,86,87]

$$(\Delta\varepsilon + A)_{ia,jb} = \Delta\varepsilon_{ia,jb} + C_{ia,jb} + [\Delta v_x]_{ia,jb} - J_{ia,jb} \tag{9}$$

$$B_{ia,jb} = C_{ia,jb} - K_{ia,jb} \tag{10}$$

DOI: 10.1021/acs.jctc.5b00024
J. Chem. Theory Comput. XXXX, XXX, XXX−XXX

with $K_{ia,jb} = [ib|ja]$ and $J_{ia,jb} = [ij|ab]$. The only difference from the TDHF Hessian is the occurrence of the Δv_x contribution, which explicitly is given by[58]

$$[\Delta v_x]_{ia,jb} = \langle i|v_x^{NL} - v_x|j\rangle\delta_{ab} - \langle a|v_x^{NL} - v_x|b\rangle\delta_{ij} \quad (11)$$

and involves differences of occupied−occupied and virtual−virtual matrix elements of the nonlocal and local exact-exchange potential, see section 2.1. It has been investigated in ref 58 that generalized TDDFT methods using the Hessian of eqs 9 and 10 yield excitation energies which are very close to corresponding TDHF excitation energies. This means, however, that local valence excitations which can be well described by standard TDDFT methods become worse with this approach. The reason for this can be attributed to the fact that the Δv_x contribution of eq 11 approximately shifts the KS orbital energy differences $\Delta\varepsilon$, which are known to yield reasonable estimates for transition energies of local excitations, to HF orbital energy differences. The latter, however, cannot describe local valence excitations well due to the fact that the unoccupied orbitals in the HF method are not self-interaction free and describe an $(N + 1)$ th-electron added to the N-electron system rather than an excited electron.[23,69]

Because of this, here different approximations to the electronic Hessian are tested by modifying the diagonal blocks (eq 9) of the Hessian matrix. Thereby it should be noted that any modification of the matrix **A** of eq 9 affects the many-body expansion of the response matrix first in second and higher orders, so that, within the framework of the adiabatic-connection fluctuation dissipation theorem (AC-FDT), correlation energies are still exact through second order with this approach.[65] The first approximation, denoted hereafter as RPAX(α = 0.0) or RPAX(0.0), is to neglect the term $\Delta\mathbf{v}_x$ and all other contributions stemming from electron exchange interactions, i.e. the matrix **J**, completely in eq 9. This means it is assumed that $\Delta\mathbf{v}_x = \mathbf{J}$ in this approximation. With this the only difference between the RPAX(0.0) Hessian and the RPA Hessian is the addition of exchange interaction contributions to the nondiagonal blocks **B** (eq 10).

It is known, however, that the approximation $\Delta\mathbf{v}_x \approx \mathbf{J}$ of the RPAX(0.0) method is not a good approximation even in case of small molecular systems. In fact, it can be shown that for the case of two-electron closed-shell systems, $\Delta\mathbf{v}_x = \mathbf{J} - \mathbf{K}$ (the first term on the right-hand-side of eq 11 vanishes in this case, and the local exchange potential equals the Coulomb potential scaled with a factor of 1/2).[64] Inserting this into eq 9 yields

$$(\Delta\varepsilon + A)_{ia,jb} = \Delta\varepsilon_{ia,jb} + C_{ia,jb} - K_{ia,jb} \quad (12)$$

which is identical to the RPAX1 method of ref 60. As compared to the original RPA approximation, eqs 6 and 7, electron exchange effects are now introduced in both the diagonal and the nondiagonal blocks of the Hessian.

Since neither the RPAX(0.0) (eqs 6 and 10) nor the RPAX1 (eq 12) Hessians, denoted hereafter as RPAX(1.0), are exact through second order in the many-body expansion of the response function, and since eq 12 holds true only for the special case of two-electron systems, in this work an interpolation between these two approaches will be tested using the following generalized form of the diagonal block of the Hessian matrix:

$$(\Delta\varepsilon + A)_{ia,jb} = \Delta\varepsilon_{ia,jb} + C_{ia,jb} - \alpha K_{ia,jb} \quad (13)$$

with α = 0 yielding the RPAX(0.0) approximation (eqs 6 and 10) and α = 1.0 the RPAX(1.0) approximation (eq 12 combined with eq 10). It has been observed that for larger molecular systems ($N_{elec} > 2$) the RPAX(1.0) approach yields excitation energies which typically strongly underestimate low-lying valence excitation energies, e.g., in the case of the pyridine molecule, the lowest $n \rightarrow \pi^*$ excitation energy, which is well described by the RPA and the RPAX(0.0) methods (4.61 and 4.57 eV, respectively, compared to the experimental value of 4.59 eV[88]), is underestimated by 1.2 eV with the RPAX(1.0) method (in all cases, the PBE0AC(BRJ) xc potential described in section 2.1 was used). Therefore, in this work, the RPAX(α) approximation was tested for a set of smaller values of α, namely α = 0.0, 0.2, and 0.5.

2.3. Long-Range Correction to the Exchange-Correlation Kernel. It is clear that the RPAX(α) approximation of eqs 13 and 10 is unable to describe long-range (charge-transfer) excitations due to the fact that the diagonal kernel contributions ($C_{ia,ia}$ and $K_{ia,ia}$) vanish if the donor orbital ϕ_i and acceptor orbital ϕ_a have a small spatial overlap with each other, i.e.

$$\phi_i(\mathbf{r})\,\phi_a(\mathbf{r}) \approx 0 \quad (14)$$

Then, in this limiting case, the excitation would solely be described by the orbital energy differences $\Delta\varepsilon$, which, if the orbital energies stem from Kohn−Sham calculations using local xc potentials, are not good approximations to charge-transfer excitations because the virtual orbital energies correspond to ionization energies and not electron affinities, see refs 23 and 70a, 70b, and section 2.1. Furthermore, even if the underlying dominant orbital pair of the excitation has a larger spatial overlap, the RPAX(α) approximation would only be able to capture the local contributions of the excitation if the two orbitals are spatially extended. In order to explain this, assume that the molecular volume is partitioned into certain domains (e.g., atomic ones) using the partitioning

$$\sum_{d}^{\text{domain}} w_d(\mathbf{r}) = 1 \quad (15)$$

so that

$$\phi_i(\mathbf{r})\,\phi_a(\mathbf{r}) = \sum_d w_d(\mathbf{r})\,\phi_i(\mathbf{r})\,\phi_a(\mathbf{r}) \quad (16)$$

then, for a domain d where $w_d(\mathbf{r})\ \phi_i(\mathbf{r})\ \phi_a(\mathbf{r}) \approx 0$, the RPAX($\alpha$) approach again would neglect electron−electron interaction contributions to the excitation (dominated by the $\phi_i \rightarrow \phi_a$ pair) even if the total spatial overlap between ϕ_i and ϕ_a is large. Evidently, such contributions can become important if the orbitals ϕ_i and ϕ_a are spatially delocalized. It should be noted that the same holds true also in the case of standard TDDFT methods employing standard local xc kernels.

A remedy to this problem is possible by taking into account the missing contributions $\Delta\mathbf{v}_x$ and **J** of eq 9 in the diagonal block of the RPAX(α) Hessian matrix (eq 13). As explained in section 2.2, the $\Delta\mathbf{v}_x$ matrix converts Kohn−Sham to Hartree−Fock orbital energies the virtual ones of which correspond to approximate electron affinities (Koopman's theorem).[69,89] In addition, the **J** term describes the Coulomb interaction between the donor and acceptor orbital densities and ensures the proper long-range dependence of the excitation energy with respect to the distance of the two spatially separated orbitals. Since in the RPAX(α) Hessian matrix, however, the contribution $\Delta\mathbf{v}_x - \mathbf{J}$ is already approximated by $-\alpha\mathbf{K}$ and in order to avoid the double

DOI: 10.1021/acs.jctc.5b00024
J. Chem. Theory Comput. XXXX, XXX, XXX−XXX

counting of electron−electron interaction effects, here only the long-range interaction contribution of $\Delta\mathbf{v}_x - \mathbf{J}$ is utilized by using

$$(\Delta\varepsilon + A)_{ia,jb} = \Delta\varepsilon_{ia,jb} + C_{ia,jb} - \alpha K_{ia,jb} + [\Delta v_x^{lr}]_{ia,jb} - J^{lr}_{ia,jb} \tag{17}$$

with

$$[\Delta v_x^{lr}]_{ia,jb} = \langle i|(v_x^{NL} - v_x)^{lr}|j\rangle\delta_{ab} - \langle a|(v_x^{NL} - v_x)^{lr}|b\rangle\delta_{ij} \tag{18}$$

and

$$J^{lr}_{ia,jb} = \left[ij\left|\frac{\zeta(r_{12})}{r_{12}}\right|ab\right] \tag{19}$$

where $\zeta(r_{12}) = 0$ for $r_{12} \to 0$ and $\zeta(r_{12}) \to 1$ for $r_{12} \to \infty$. In this work, the function $\zeta(r_{12}) = \mathrm{erf}(\beta r_{12})$ is used, which is widely used also in range-separated density-functional methods due to the fact that integrals for the erf interaction can efficiently be calculated for Gaussian-type basis functions.[90] In eq 18, the superscript *lr* means that both the local and nonlocal exchange potentials are too calculated for the long-range Coulomb interaction $\zeta(r_{12})/r_{12}$ instead of the full-range interaction $1/r_{12}$. This means that the OEP eq 2 is solved with the substitution:

$$\langle\phi_i|v_x^{NL}|\phi_a\rangle \to \langle\phi_i|(v_x^{NL})^{lr}|\phi_a\rangle = -\sum_k^{occ}\left[\phi_i\phi_k\left|\frac{\zeta(r_{12})}{r_{12}}\right|\phi_k\phi_a\right] \tag{20}$$

Other technical details of the OEP, e.g. the use of additional constraints in the solution, are identical to those described in section 2.1.

The long-range correction of eqs 17−19 adds another parameter to the Hessian matrix, namely the parameter β of the long-range Coulomb potential $v_J^{lr}(r_{12}) = \mathrm{erf}(\beta r_{12})/r_{12}$. Other than in range-separated methods where the short-range contributions are described with the corresponding complementary short-range Coulomb potential $v_J^{sr}(r_{12}) = (1 - \mathrm{erf}(\beta r_{12}))/r_{12}$, here the short-range exchange contributions are accounted for completely by the particle-hole contributions in the diagonal (eq 17) and nondiagonal (eq 10) parts of the Hessian. Because of this, the value of β has to be small enough in order to yield only small contributions to local excitation energies. On the other hand, even in the case of local excitations one can find small or even vanishing contributions of the particle-hole type Hessian matrix elements due to the symmetry of the contributing orbital pairs. A method to distinguish such excitations from Rydberg excitations, which too are local, is to measure the ratio $\langle\phi_a|r^2|\phi_a\rangle/\langle\phi_i|r^2|\phi_i\rangle$ of the radial expectation values for the dominating occupied−virtual orbital pairs of the excitation. In the case of Rydberg excitations, this term usually exceeds a value of 4.0 because the virtual Rydberg orbital ϕ_a is much more diffuse than the valence orbital ϕ_i. With this diagnostic, in this work, two excitations could be segregated which are local non-Rydberg excitations with a small spatial overlap of the contributing orbital pairs: the first $\pi \to \pi^*$ excitation in pyridine (B_2 symmetry) and the third $n \to \pi^*$ excitation in pyrazine (B_{1g} symmetry). In these two cases, it has been found that the RPA or RPAX(α) Hessian corrections only marginally affect the uncoupled contribution $\Delta\varepsilon$ to the excitation energy. However, in both cases, the uncoupled excitation energy (using the PBE0AC(BRJ) xc potential) underestimates the experimental values, in the case of pyridine by a magnitude of 0.8 eV and in the case of pyrazine by 0.4 eV. Since both excitations are affected by the long-range correction of eq 17, they have been used in order to obtain proper values for the range parameter β. With this and the above-mentioned condition that this value should be not too large to not also affect short-range excitations with stronger spatial overlaps of the contributing occupied-virtual orbital pairs, it was found that the setting $\beta = 0.2$ is reasonable. By this, the error for the $n \to \pi^*$ excitation in pyrazine could be removed completely, while in the case of the $\pi \to \pi^*$ excitation in pyridine the error reduces to about 0.57 eV, see section 4.1.

In the following, the long-range correction approach described in this section will be termed as RPAXerfJ(α,β). Since it has been tested only in conjunction with the RPAX(α = 0.2) Hessian, the abbreviation RPAXerfJ($\alpha = \beta = 0.2$), RPAXerfJ(0.2), will be used in the following.

2.4. Transformation to Casida Eigenvalue Equation Form. The solutions of the generalized eigenvalue equation (assuming real-valued orbitals)

$$\left[\begin{pmatrix}\Delta\varepsilon & \mathbf{0}\\ \mathbf{0} & \Delta\varepsilon\end{pmatrix} + \begin{pmatrix}\mathbf{A} & \mathbf{B}\\ \mathbf{B} & \mathbf{A}\end{pmatrix}\right]\begin{pmatrix}\mathbf{X}_p\\ \mathbf{Y}_p\end{pmatrix} = \omega_p\begin{pmatrix}-\mathbf{1} & \mathbf{0}\\ \mathbf{0} & \mathbf{1}\end{pmatrix}\begin{pmatrix}\mathbf{X}_p\\ \mathbf{Y}_p\end{pmatrix} \tag{21}$$

are paired; that is, if $(\mathbf{X}_p\ \mathbf{Y}_p)^T$ is an eigenvector corresponding to an eigenvalue ω_p, then $(\mathbf{Y}_p\ \mathbf{X}_p)^T$ is an eigenvalue corresponding to the negative eigenvalue $-\omega_p$. Because of this, there is a redundancy if the complete spectrum of eq 21 is calculated. It can be shown, however, that eq 21 can be transformed to a nonsymmetric eigenvalue equation that has only half the dimension (of $N_{occ} \times N_{vir}$) but in which the solutions are the squared excitation energies:[86,87]

$$(\Delta\varepsilon + \mathbf{A} - \mathbf{B})(\Delta\varepsilon + \mathbf{A} + \mathbf{B})\mathbf{U}_p = \omega_p^2\mathbf{U}_p \tag{22}$$

This equation differs from the Casida equation of TDDFT which is given by the symmetric eigenvalue equation[4,91]

$$(\Delta\varepsilon^2 + \Delta\varepsilon^{1/2}\mathbf{K}\Delta\varepsilon^{1/2})\mathbf{Z}_p = \omega_p^2\mathbf{Z}_p \tag{23}$$

with

$$\mathbf{K} = 2\mathbf{C} + \mathbf{F}_{xc} \tag{24}$$

being the coupling matrix containing the Coulomb matrix and the xc kernel matrix (stemming from a generally nonadiabatic and nonlocal xc kernel $f_{xc}(\mathbf{r}_1,\mathbf{r}_2,\omega)$).

It will now be shown that eq 22 can be transformed into the Casida form of eq 23 under the assumption that the matrix $\Delta\varepsilon^{-1/2}(\mathbf{A} - \mathbf{B})\Delta\varepsilon^{-1/2}$ is small compared to the unit matrix, more correctly, for which it holds true that $\kappa_{ia} \ll 1$ for all eigenvalues κ_{ia} of this matrix. For this, eq 22 is transformed into the symmetric generalized eigenvalue equation

$$(\Delta\varepsilon + \mathbf{K}_1)\mathbf{U}_p = \omega_p^2(\Delta\varepsilon + \mathbf{K}_2)^{-1}\mathbf{U}_p \tag{25}$$

using the abbreviations $\mathbf{K}_1 = \mathbf{A} + \mathbf{B}$ and $\mathbf{K}_2 = \mathbf{A} - \mathbf{B}$. Exploiting the diagonal form of $\Delta\varepsilon$, this equation can be transformed into

$$(\Delta\varepsilon^2 + \Delta\varepsilon^{1/2}\mathbf{K}_1\Delta\varepsilon^{1/2})\tilde{\mathbf{U}}_p = \omega_p^2(\mathbf{1} + \Delta\varepsilon^{-1/2}\mathbf{K}_2\Delta\varepsilon^{-1/2})^{-1}\tilde{\mathbf{U}}_p \tag{26}$$

DOI: 10.1021/acs.jctc.5b00024
J. Chem. Theory Comput. XXXX, XXX, XXX−XXX

The inverse of the matrix on the right-hand side of this equation can be expanded as follows:

$$(\mathbf{1} + \Delta\varepsilon^{-1/2}\mathbf{K}_2\Delta\varepsilon^{-1/2})^{-1} \approx \mathbf{1} - \Delta\varepsilon^{-1/2}\mathbf{K}_2\Delta\varepsilon^{-1/2} + \Delta\varepsilon^{-1/2}\mathbf{K}_2\Delta\varepsilon^{-1}\mathbf{K}_2\Delta\varepsilon^{-1/2} - \ldots \quad (27)$$

Insertion in eq 26 and rearrangement of terms gives

$$(\Delta\varepsilon^2 + \Delta\varepsilon^{1/2}[\mathbf{K}_1 + \omega^2(\Delta\varepsilon^{-1}\mathbf{K}_2\Delta\varepsilon^{-1} - \Delta\varepsilon^{-1}\mathbf{K}_2\Delta\varepsilon^{-1}\mathbf{K}_2\Delta\varepsilon^{-1} + \ldots)]\Delta\varepsilon^{1/2})\mathbf{Z}_p = \omega_p^2\mathbf{Z}_p \quad (28)$$

where it has been implied that the first- and higher order terms on the right-hand side of eq 26 depend explicitly on the general frequency ω. As can be seen, eq 28 is now of the same form as the Casida eq 23. This means that the xc kernel matrix of eq 24 is given by

$$\mathbf{F}_{xc} = \mathbf{K}_1 - 2\mathbf{C} + \omega^2(\Delta\varepsilon^{-1}\mathbf{K}_2\Delta\varepsilon^{-1} - \Delta\varepsilon^{-1}\mathbf{K}_2\Delta\varepsilon^{-1}\mathbf{K}_2\Delta\varepsilon^{-1} + \ldots) \quad (29)$$

and thus is both nonlocal and frequency dependent. The latter means that the solutions of eq 28 are given by the intersection points of the functions $\omega_p(\omega)$ with $f(\omega) = 1$ for each excited state p depending on the frequency ω.

Considering now the explicit form for the coupling matrices $\mathbf{K}_1$ and $\mathbf{K}_2$ given by the RPAX(α) and RPAXerfJ(α,β) methods described in sections 2.2 and 2.3, it can be seen that the RPAX(1.0) (=RPAXerfJ(1.0,0.0)) method corresponds to the adiabatic form of eq 29; i.e., the exchange-kernel within the RPAX(1.0) approximation does not depend on the frequency. In contrast to this, the RPAXerfJ(0.0,∞) method is identical to the TDEXX method of refs 28, 58, and 65 if the quadratic and higher order frequency-dependent terms in eq 29 are neglected. Thus, the RPAXerfJ(α,β) method of section 2.3 can be considered as an interpolation between the RPAX(1.0) method (termed RPAX1 in ref 60) and the full TDEXX method for values of $\alpha < 1.0$ and any finite value of β.

2.5. Summary of Methods Used. In this section, the acronyms for the different methods used in this work are briefly reviewed.

For the ground-state Kohn–Sham calculations, the following approximations for the xc potential have been used:

PBE0AC(EXX) localized and asymptotically corrected PBE0 xc potential in which the nonlocal exact exchange potential is replaced by the local EXX potential, eqs 4 and 2

PBE0AC(BRJ) localized and asymptotically corrected PBE0 xc potential in which the nonlocal exact exchange potential is replaced by the local BRJ potential, eqs 4 and 3

For the time-dependent DFT calculations, the Hessian matrices were approximated by the methods:

RPA: random-phase approximation. Only direct Coulomb interactions are accounted for in the contributions to the Hessians (eqs 6 and 7)

RPAX(α): random-phase approximation including exchange interactions. In addition to the RPA, also exchange particle–hole interactions are accounted for (eqs 13 and 10). The parameter α denotes a constant scaling factor in the diagonal blocks of the Hessian, eq 13. In this work, this parameter was set to values of α = 0.0, 0.2, and 0.5.

RPAXerfJ(α,β): the RPAX(α) Hessian approximation is augmented by long-range particle–particle/hole–hole interaction contributions, see eq 17. The range-separation parameter β (see section 2.3) was set to 0.2 in this work.

ALDA: The RPA Hessian is corrected by the standard ALDA kernel, eq 8.

3. COMPUTATIONAL DETAILS

Excitation energies with the methods described in sections 2.1–2.3 were calculated for the 11 molecules from the TDDFT benchmark of Caricato et al.[31] comprising three alkene molecules (ethylene, t-butadiene, and isobutene), three carbonyl molecules (formaldehyde, acetaldehyde, and acetone), and five azabenzenes (pyridine, pyrazine, pyrimidine, pyridazine, and S-tetrazine). The reference excitation energies of this benchmark are all taken from experiments in the gas phase, see ref 31 and references therein. Almost all experimental transitions were corrected by removing the adiabatic effects to match vertical excitations (e.g., using the intensity weighted average energy of the transition instead of the band maxima). High-accuracte ab initio results of excitation energies for some of the molecules[92] indicate that the experimental (gas-phase) excitation energies corrected in this way have errors of not more than about ±0.1 eV to the actual vertical excitation energies. Concerning the assignment of the individual transitions, the same technique as reported in ref 31 has been applied. In addition, in order to test particularly the accuracy of the RPAXerfJ(0.2) method for describing long-range charge-transfer excitations, excitation energies were calculated for a selection of four molecules from a work of Peach et al.,[35,93] namely *N*-phenylpyrrole (PP), and the three model polypeptides of ref 94. The geometries for all molecules were taken from refs 31 and 35, respectively.

In order to properly describe both, Rydberg and valence excitations, the doubly augmented quadruple-ζ (d-aug-cc-pVQZ) basis set of Dunning et al.[95−97] has been used in the calculations of the molecules from the Caricato benchmark, truncated, however, to *s*- and *p*-functions on hydrogen and *s*-, *p*-, and *d*-functions on carbon, oxygen, and nitrogen. It has been observed that this basis set truncation did almost have no effect on the considered low-lying excitation energies. In the case of the molecules from the work of Peach et al.,[35] the cc-pVTZ basis set by Dunning[95] has been utilized in order to enable a direct comparison with the other TDDFT and correlated wave function results of refs 35 and 93.

In all cases, the excitation energies were obtained by solving the reduced hermitian eigenvalue equation for the squared excitation energies ω_p^2

$$(\Delta\varepsilon + \mathbf{A} - \mathbf{B})^{1/2}(\Delta\varepsilon + \mathbf{A} + \mathbf{B})(\Delta\varepsilon + \mathbf{A} - \mathbf{B})^{1/2}\mathbf{U}_p = \omega_p^2\mathbf{U}_p \quad (30)$$

with the matrices $\Delta\varepsilon$, $\mathbf{A}$, and $\mathbf{B}$ defined in the sections 2.2 and 2.3. Since in this work the Hessian matrices do not originate from a direct functional derivative of the underlying energy functional, two types of instabilities in the solution of eq 30 have to be taken into account, namely the singlet instability and the nonreal instability. The singlet instability arises when the matrix $\Delta\varepsilon + \mathbf{A} + \mathbf{B}$ possesses a negative eigenvalue while a nonreal instability occurs when the matrix $\Delta\varepsilon + \mathbf{A} - \mathbf{B}$ has a negative eigenvalue (so that it is not possible to take the square-root of this matrix). It has been observed that such instabilities did not occur for all excitations considered in this work.

DOI: 10.1021/acs.jctc.5b00024
J. Chem. Theory Comput. XXXX, XXX, XXX−XXX

The Kohn−Sham molecular orbitals and orbital eigenvalues have been calculated using the xc potentials described in section 2.1. These potentials were corrected in the asymptotic range by using the OEP-AC method and employing the derivative-discontinuity correction shifts for the HOMO condition. For this, the ionization energies of each molecule have been calculated in advance from the total energies for the neutral and cationic system using the PBE0[68] xc functional in the KS calculations. The results for the ionization energies are displayed in Table 1.

Table 1. Ionization Energies Calculated with the PBE0 xc Functional (def2-TZVP Basis, values in au)

molecule	E_{IP}
ethylene	0.384
isobutene	0.336
t-butadiene	0.323
formaldehyde	0.396
acetaldehyde	0.370
acetone	0.351
pyridine	0.350
pyrazine	0.352
pyrimidine	0.353
pyridazine	0.336
S-tetrazine	0.357
PP	0.295
dipeptide	0.334
β-dipeptide	0.327
tripeptide	0.325

Electrostatic potential functions of standard Gaussian functions were used to expand the local exchange potential in the OEP, see ref 78. In this work, the aug-cc-pVQZ-MP2Fit basis set by Weigend et al.[98] was used for the Gaussian basis set. In order to improve the numerical stability in the solution to the OEP equation, a small amount of the Coulomb kernel matrix has been added to the response matrix:

$$\tilde{\mathbf{X}}_0 = \mathbf{X}_0 + \lambda \mathbf{J} \tag{31}$$

The parameter λ in eq 31 was chosen such that the EXX potential matches corresponding accurate EXX potentials obtained with the OEP method of ref 78. The optimized value of λ obtained in this way was $\lambda = 3 \times 10^{-4}$. In addition, both the HOMO and charge constraints as decribed in ref 78 were used in the OEP to improve the numerical stability. To test the influence of the variation of the OEP auxiliary basis set on the excitation energies, the larger aug-cc-pV5Z-MP2Fit basis set[98] has been used in combination with the same orbital basis set for some systems using the PBE0AC(EXX) xc potential. The resulting excitation energies did not differ more than 0.02 eV on average from the results with the smaller auxiliary basis set, proving that the regularization approach of eq 31 ensures numerical stability even with large auxiliary basis sets.

All calculations were performed using a developers version of the Molpro quantum chemistry program.[99,100] For comparison, standard TDDFT calculations were done for the pyridine molecule using the Turbomole program.[101]

4. RESULTS

4.1. Excitation Energies for Alkenes, Carbonyls, and Azabenzenes. The calculated excitation energies for the alkenes, carbonyls, and azabenzenes are shown in the Tables 2,

Table 2. Excitation Energies of Alkenes (in eV)[a]

molecule	excitation		RPA	RPAX α = 0.0	RPAX α = 0.2	RPAX α = 0.5	ALDA	RPAXerfJ α,β = 0.2	exp.
ethylene	$1B_{3u}$	Ryd	7.15	7.15	7.14	7.12	7.02	7.27	7.11
	$1B_{1u}$	$\pi\rightarrow\pi^*$	7.71	7.70	7.71	7.70	7.62	7.86	7.80
	$1B_{1g}$	Ryd	7.71	7.72	7.71	7.70	7.63	7.93	7.90
	$1B_{2g}$	Ryd	8.03	8.39	8.15	7.62	7.60	8.08	7.65
	$2A_g$	Ryd	8.36	8.36	8.33	8.29	8.21	8.32	8.28
	$2B_{3u}$	Ryd	8.59	8.59	8.59	8.58	8.52	8.68	8.62
	$3B_{3u}$	Ryd	8.93	8.93	8.93	8.92	8.83	8.96	8.90
	$4B_{3u}$	Ryd	9.11	9.11	9.10	9.09	9.04	9.12	9.08
	$3B_{1g}$	Ryd	9.18	9.18	9.18	9.17	9.15	9.21	9.20
	$2B_{1u}$	Ryd	9.25	9.36	9.27	9.17	9.16	9.25	9.33
	$5B_{3u}$	Ryd	9.74	9.74	9.74	9.73	9.70	9.82	9.51
isobutene	B_1	Ryd	5.82	5.82	5.81	5.80	5.74	6.19	6.17
	A_1	Ryd	6.56	6.63	6.59	6.46	6.40	6.75	6.70
t-butadiene	$1B_u$	$\pi\rightarrow\pi^*$	5.74	6.08	5.89	5.49	5.50	5.97	5.91
	$1B_g$	Ryd	5.96	5.95	5.95	5.94	5.88	6.13	6.22
	$2A_u$	Ryd	6.29	6.29	6.29	6.27	6.21	6.57	6.66
	$2B_u$	Ryd	6.94	7.02	6.95	6.87	6.85	6.96	7.07
	$2B_g$	Ryd	7.00	7.00	7.00	6.99	6.95	7.20	7.36
	$3A_g$	Ryd	7.43	7.45	7.43	7.30	7.31	7.49	7.62
	$3B_u$	Ryd	7.95	7.95	7.95	7.95	7.92	7.95	8.00
MAE			0.16	0.17	0.16	0.17	0.21	0.10	
MAX			0.38	0.74	0.50	0.42	0.45	0.43	

[a]The last two lines in the table show the mean absolute error (MAE) and the maximum error (MAX) of the respective methods.

DOI: 10.1021/acs.jctc.5b00024
J. Chem. Theory Comput. XXXX, XXX, XXX−XXX

Table 3. Excitation Energies of Carbonyls (in eV)[a]

molecule	excitation		RPA	RPAX α = 0.0	RPAX α = 0.2	RPAX α = 0.5	ALDA	RPAXerfJ α,β = 0.2	exp.
formaldehyde	$1A_2$	$n\rightarrow\pi^*$	4.23	4.13	4.08	3.96	3.96	3.99	4.00
	$1B_2$	Ryd	7.04	7.05	7.03	7.01	6.85	7.22	7.08
	$2B_2$	Ryd	7.89	7.89	7.88	7.86	7.74	8.02	7.97
	$2A_1$	Ryd	8.03	8.04	8.02	7.99	7.87	8.15	8.14
	$2A_2$	Ryd	8.30	8.30	8.30	8.30	8.25	8.36	8.37
	$3B_2$	Ryd	8.93	8.94	8.92	8.91	8.83	9.00	8.88
	$1B_1$	$\pi\rightarrow\pi^*$	9.17	9.17	9.17	9.16	9.12	9.20	9.26
	$3A_2$	Ryd	9.25	9.35	9.32	9.30	9.21	9.40	9.00
acetaldehyde	A″	$n\rightarrow\pi^*$	4.52	4.40	4.36	4.24	4.28	4.23	4.28
	2A′	Ryd	7.09	7.10	7.09	7.06	6.95	7.38	6.82
	3A′	Ryd	7.50	7.50	7.49	7.46	7.40	7.66	7.46
	4A′	Ryd	8.00	8.00	7.98	7.93	7.90	8.27	7.75
	6A′	Ryd	8.41	8.41	8.40	8.40	8.34	8.53	8.43
	7A′	Ryd	8.59	8.60	8.55	8.62	8.61	8.66	8.69
acetone	$1A_2$	$n\rightarrow\pi^*$	4.60	4.49	4.45	4.34	4.39	4.33	4.43
	$1B_2$	Ryd	5.71	5.71	5.70	5.69	5.66	6.21	6.36
	$2A_2$	Ryd	6.79	6.79	6.76	6.71	6.73	7.24	7.41
	$2A_1$	Ryd	6.87	6.87	6.86	6.86	6.84	7.19	7.36
	$2B_2$	Ryd	7.06	7.06	7.06	7.05	7.00	7.31	7.49
	$3A_1$	Ryd	7.24	7.24	7.23	7.21	7.19	7.62	8.09
	$3B_2$	Ryd	7.66	7.66	7.65	7.64	7.58	7.93	7.80
	$1B_1$	Ryd	7.74	7.74	7.74	7.74	7.71	8.02	8.17
MAE			0.24	0.23	0.22	0.22	0.24	0.16	
MAX			0.85	0.85	0.86	0.88	0.90	0.56	

[a]The last two lines in the table show the mean absolute error (MAE) and the maximum error (MAX) of the respective methods.

3, and 4 using the different approximations for the Hessian matrix described in the sections 2.2 and 2.3 and the PBE0AC(BRJ) xc potential, see section 2.1. The experimental (vertical) reference values for each excitation are displayed in the last column and are taken from refs 102 (ethylene, formaldehyde and acetone); 103 (t-butadiene); 104 (acetaldehyde); 88, 92, 105, and 106 (pyridine); 92, 105, and 107 (pyrazine and pyrimidine); 92 and 108 (pyridazine); and 92, 107, and 109−113 (S-tetrazine). (Note that as in the work of Caricato et al.[31] the 2^1A_g excitation of t-butadiene has been omitted because its assignment is controversial[104]). It can be seen that the low lying excitations of the alkene and carbonyl molecules are dominantly of Rydberg character while in case of the azabenzenes all lowest excitations are either of $n \rightarrow \pi^*$ or $\pi \rightarrow \pi^*$ character. Because of this, the excitation energies for the alkenes and carbonyls mainly serve for assessing the accuracy of the underlying xc potential while the excitation energies for the azabenzenes are more strongly affected also by the approximations of the Hessian.

One can observe that (with only few exceptions) in the case of the Rydberg excitations of the alkenes and carbonyls, Tables 2 and 3, the excitation energies obtained by the RPA, RPAX(α), and ALDA approximations hardly differ from each other. This indicates that, as expected, the xc kernel in these cases gives only a small correction to the uncoupled (single-particle) excitations. In contrast to this, the RPAXerfJ(0.2) approximation yields Rydberg excitations which deviate more strongly from the RPA excitation energies. While one can see that this deviation is always positive, see Tables 2 and 3, in a number of cases this leads to a very good agreement with the experimental reference values. For example, for isobutene (Table 2) the RPA, RPAX(α), and ALDA TDDFT methods underestimate the lowest experimental transition by almost 0.4 eV, while the RPAXerfJ(0.2) method slightly overestimates the experimental value of 6.17 eV by 0.02 eV only.

A comparison of the excitation energies from the different exchange variants RPAX(0.0), RPAX(0.2), and RPAX(0.5) to the RPA excitation energies shows that even in case of valence excitations, i.e. excitations for which one may expect a stronger correction to the single-particle excitations, the differences are quite small, especially for the RPAX(0.0) approximation, see Tables 2, 3, and 4. This is also indicated by the respective mean and maximum absolute errors for each group shown in the two final lines in each table. A comparison of the RPAX(α) excitation energies among each other shows that the increase of the value of α (cf. eq 13) generally leads to a decrease of the transition energy, usually on the order of 0.1 to 0.2 eV. In some cases, however, the decrease in the excitation energy when varying the value of α from 0.0 to 0.5 can be quite strong; e.g., in the case of the second $B_1(n \rightarrow \pi^*)$ excitation of pyrimidine, the excitation energies for RPAX(α = 0.0, 0.2, 0.5) are 5.58, 5.22, and 4.65 eV, respectively (see Table 4). Since the experimental reference result equals 5.12 eV in this case, the RPAX(0.5) strongly underestimates the second $B_1(n \rightarrow \pi^*)$ excitation energy of pyrimidine. In many cases where the variation of α has a strong effect on the calculated excitation energies, it is found that the RPAX(0.0) results usually overestimate the respective experimental values and that the RPAX(0.2) approach reduces these deviations strongly. Examples for this are observed for t-butadiene/$\pi \rightarrow \pi^*$ (Table 2), pyridine/A_2, pyrazine/B_{2g} and B_{1u}, pyrimidine/A_1, and pyridazine/A_2 (Table 4). This is also reflected in the mean

DOI: 10.1021/acs.jctc.5b00024
J. Chem. Theory Comput. XXXX, XXX, XXX−XXX

Table 4. Excitation Energies of Azabenzenes (in eV)[a]

molecule	excitation		RPA	RPAX α = 0.0	RPAX α = 0.2	RPAX α = 0.5	ALDA	RPAXerfJ α,β = 0.2	exp.
pyridine	$1B_1$	$n\rightarrow\pi^*$	4.61	4.57	4.53	4.43	4.47	4.80	4.59
	$1B_2$	$\pi\rightarrow\pi^*$	5.47	5.32	4.97	4.41	5.34	4.99	4.99
	$1A_2$	$n\rightarrow\pi^*$	4.65	4.59	4.59	4.55	4.59	4.86	5.43
	$1A_1$	$\pi\rightarrow\pi^*$	6.50	6.66	6.24	5.51	6.21	6.38	6.38
pyrazine	$1B_{3u}$	$n\rightarrow\pi^*$	3.81	3.77	3.72	3.61	3.65	3.94	3.83
	$1B_{2u}$	$\pi\rightarrow\pi^*$	5.39	5.36	5.31	5.20	5.23	5.63	5.46
	$1B_{2g}$	$n\rightarrow\pi^*$	5.39	5.30	4.94	4.36	5.23	4.92	4.81
	$1B_{1g}$	$n\rightarrow\pi^*$	5.77	5.74	5.74	5.71	5.73	6.10	6.10
	$1B_{1u}$	$\pi\rightarrow\pi^*$	6.75	6.93	6.50	5.73	6.43	6.60	6.51
pyrimidine	$1B_1$	$n\rightarrow\pi^*$	4.01	3.95	3.93	3.85	3.89	4.17	3.85
	$1A_2$	$n\rightarrow\pi^*$	4.22	4.15	4.13	4.08	4.14	4.37	4.62
	$1B_2$	$\pi\rightarrow\pi^*$	5.30	5.27	5.24	5.15	5.19	5.61	5.52
	$2A_2$	$n\rightarrow\pi^*$	5.53	5.50	5.48	5.42	5.44	5.80	5.90
	$2B_1$	$n\rightarrow\pi^*$	5.72	5.58	5.22	4.65	5.59	5.23	5.12
	$1A_1$	$\pi\rightarrow\pi^*$	6.77	6.91	6.52	5.77	6.47	6.66	6.70
pyridazine	$1B_1$	$n\rightarrow\pi^*$	3.37	3.36	3.31	3.21	3.24	3.55	3.60
	$1A_1$	$\pi\rightarrow\pi^*$	5.29	5.21	5.18	5.07	5.14	5.44	5.30
	$1A_2$	$n\rightarrow\pi^*$	5.59	5.44	5.07	4.48	5.47	5.09	5.00
	$2B_1$	$n\rightarrow\pi^*$	5.64	5.60	5.59	5.54	5.56	5.92	6.00
	$1B_2$	$\pi\rightarrow\pi^*$	6.62	6.76	6.31	5.56	6.31	6.47	6.50
S-tetrazine	$1B_{3u}$	$n\rightarrow\pi^*$	2.09	2.07	2.03	1.92	1.96	2.22	2.25
	$1A_u$	$n\rightarrow\pi^*$	3.07	2.99	2.97	2.92	2.98	3.27	3.40
	$2A_u$	$n\rightarrow\pi^*$	4.85	4.77	4.73	4.62	4.71	5.01	5.00
	$2B_{3u}$	$n\rightarrow\pi^*$	5.85	5.82	5.80	5.75	5.76	6.15	6.34
MAE			0.29	0.32	0.25	0.49	0.33	0.12	
MAX			0.78	0.84	0.84	0.94	0.84	0.57	

[a]The last two lines in the table show the mean absolute error (MAE) and the maximum error (MAX) of the respective methods.

absolute errors for the azabenzene group of molecules with values of 0.32, 0.25, and 0.49 eV for the RPAX(0.0), RPAX(0.2), and RPAX(0.5) methods, respectively.

Results for the ALDA xc kernel have been included in the Tables 2, 3, and 4 in order to analyze the difference between excitation energies from local and nonlocal xc kernels and to be able to compare the results with standard TDDFT methods (see section 4.2). While for the alkene and carbonyl group of systems the results are again close to the RPA and RPAX(α) excitation energies because of the dominating Rydberg character, for the azabenzene molecules one can observe that $n \rightarrow \pi^*$ excitations with the ALDA kernel are often more close to those from the RPAX(0.0) method while $\pi \rightarrow \pi^*$ excitations are smaller in magnitude than the corresponding values of the RPAX(0.0) method and thus more close to the RPAX(0.2) excitation energies, see e.g. the A_1 and A_2 excitations of pyridine or the A_2 and B_2 excitations of pyridazine in Table 4. The overall performance of the ALDA method is similar to that of the RPAX(0.0) method that is worse compared to the RPAX(0.2) excitation energies.

Because of the fact that the RPAX(α = 0.2) approximation yields the best agreement with the experimental reference excitation energies for the considered molecules, the RPAXerfJ-(α,β) approach (eqs 17 and 10) in this work was tested in conjunction with the settings α = 0.2 and β = 0.2 (see section 2.3 regarding the choice for the value of the parameter β). As already noted above, the long-range correction of eq 17 gives a nonnegligible contribution already for the low-lying excitation energies of the small molecules considered in this work. While this contribution is always positive compared to the RPAX(0.2) excitation energies, the resulting excitation energies by this are often shifted close toward the experimental values. Examples for this are found for pyrazine/B_{1g}, pyrimidine/$2A_2$, or S-tetrazine/$2A_u$. Due to this trend, the RPAXerfJ(0.2) excitation energies yield the best agreement with the experimental results for all Hessian approximations studied in this work with MAEs of 0.10, 0.16, and 0.12 eV for the alkene, carbonyl, and azabenzene group of molecules, see Tables 2, 3, and 4.

Figure 1 shows a summary of the errors of the excitation energies for the individual Hessian approximations (excluding the RPAX(0.0) and RPAX(0.5) approaches) using the PBE0AC(BRJ) and PBE0AC(EXX) xc potentials. Precisely, the diagram in Figure 1 shows the mean absolute errors for all states, the maximum errors for all states, the mean absolute errors for the respective first states, and the mean absolute errors for the combined alkene and carbonyl group of molecules and the azabenzenes. It can be seen that generally the errors of the excitation energies from the PBE0AC(BRJ) and PBE0AC(EXX) xc potentials deviate only slightly from each other so that it can be concluded that the differences in the exchange part of both potentials are small. However, if the average errors for the lowest excitations are considered, see Figure 1, it is apparent that the ones using the PBE0AC(BRJ) xc potential are consistently smaller than with the PBE0AC-

DOI: 10.1021/acs.jctc.5b00024
J. Chem. Theory Comput. XXXX, XXX, XXX−XXX

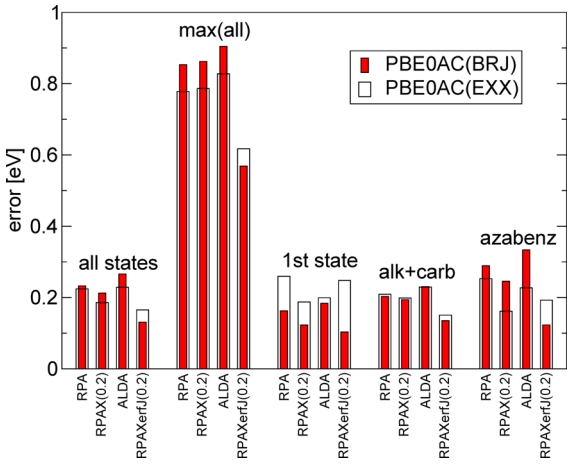

Figure 1. Comparison between the PBE0AC(BRJ) and PBE0AC(EXX) xc potentials with respect to the errors yielded by the different Hessian approximations.

(EXX) xc potential, irrespective of the choice for the Hessian matrix. To explain this finding, the HOMO−LUMO gaps of the considered molecules obtained with the PBE0AC(EXX) and PBE0AC(BRJ) were compared with each other. It has been found that the ones yielded by the PBE0AC(BRJ) are always smaller by about 0.2 eV on average than the gaps of the PBE0AC(EXX) method, and therefore it can be expected that this actually causes the difference between the coupled excitation energies obtained with both xc potentials. When all excitations are considered, however, the PBE0AC(EXX) xc potential yields smaller errors than the PBE0AC(BRJ) xc potential. The only exception for this is found for the RPAXerfJ(0.2) Hessian approximation for which the errors with the PBE0AC(BRJ) xc potential are smaller on average.

4.2. Comparison to Standard Wave Function and TDDFT Methods. In order to compare the calculated excitation energies for the TDDFT benchmark database of Caricato et al.[31] to standard methods, Figure 2 displays the mean absolute errors for the RPA, RPAX(0.2), and

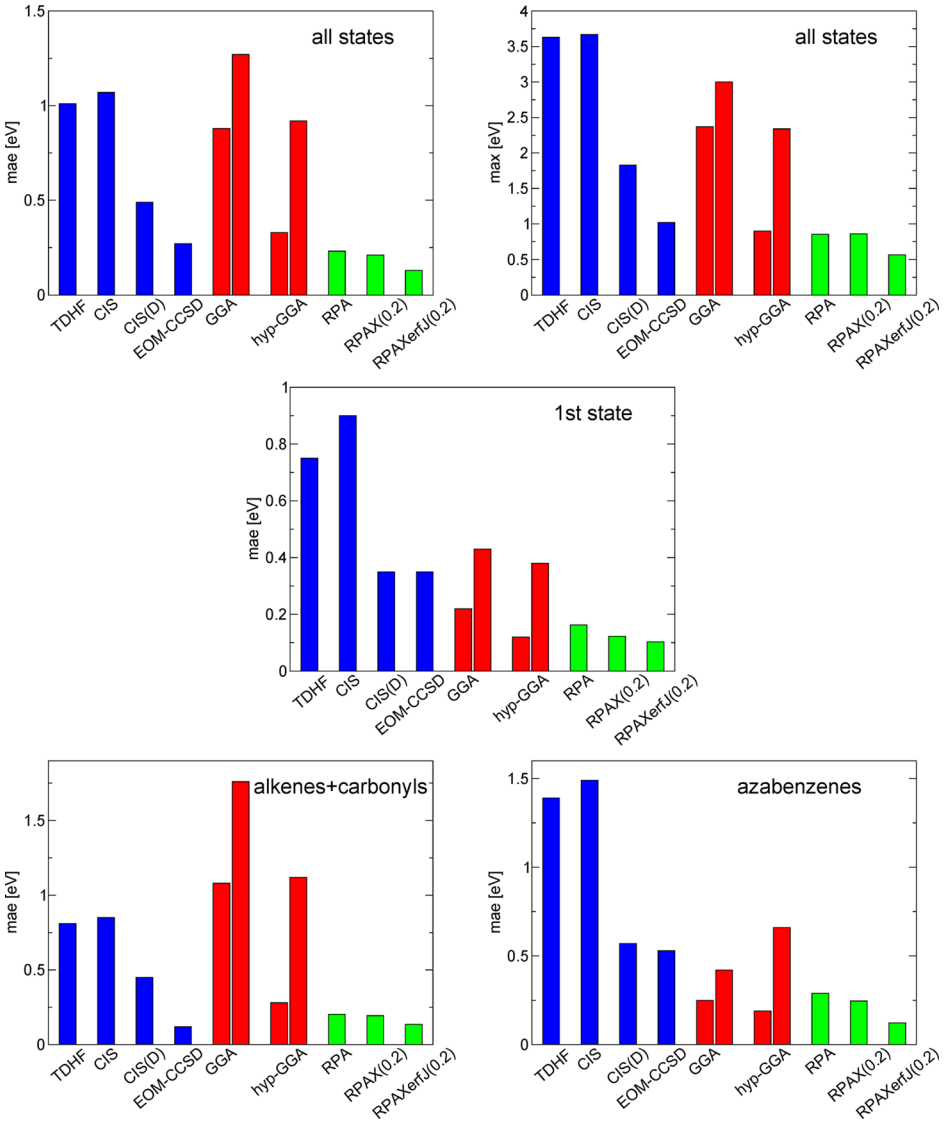

Figure 2. Mean (mae) and maximum (max) absolute errors to the experiment of the excitation energies of different wave function methods (blue bars), GGA and hyper-GGA functionals (red bars), and the RPA and exchange-RPA methods of this work (green bars). The values for the wave function and standard DFT methods are taken from ref 31. In the case of the GGA and hyper-GGA values, the errors for the respective best and worst functional for the considered group of excitations is presented.

DOI: 10.1021/acs.jctc.5b00024
J. Chem. Theory Comput. XXXX, XXX, XXX−XXX

RPAXerfJ(0.2) approximations (using the PBE0AC(BRJ) xc potential) along with those from other wave function and TDDFT methods considered in ref 31. These are time-dependent Hartree−Fock (TDHF), configuration-interaction singles (CIS), CIS including double excitations (CIS(D)), equation-of-motion coupled-cluster singles and doubles (EOM-CCSD), and a range of generalized-gradient approximation (GGA) and hyper-GGA functionals. The GGA group of functionals (containing also meta-GGA functionals) thereby comprises LDA, BLYP, OLYP, BP86, BVP86, PBE, HCTH, τ-HCTH, BB95, VSXC, and TPSS while the hyper-GGA group of functionals (containing also range-separated functionals) include O3LYP, B3LYP, B3P86, B3VP86, PBE0, B1B95, τ-HCTH-hyb, TPSS-hyb, M05, BH&H, BH&HLYP, BMK, M05-2X, HSE1PBE, CAM-B3LYP, LC-BLYP, and LC-ωPBE, see Table 1 of ref 31 for references of the respective functionals. Note that in the diagrams in Figure 2 in the case of the GGA and hyper-GGA functionals, the respective lower bar shows the error for the functional of the given group with the smallest error to the experimental reference results, while the larger bar shows the error for the functional having the largest error.

For a direct comparison of the results of this work to the benchmark values of the work of Caricato et al.,[31] one should distinguish between the performance of the xc potential and the xc kernels used in this work. For this, it should be noted that excitation energies calculated with different adiabatic and local approximations of the xc kernel but with the same xc potential for the ground-state calculations are very close to each other. As an example, Figure 3 shows the lowest excitation energies of the

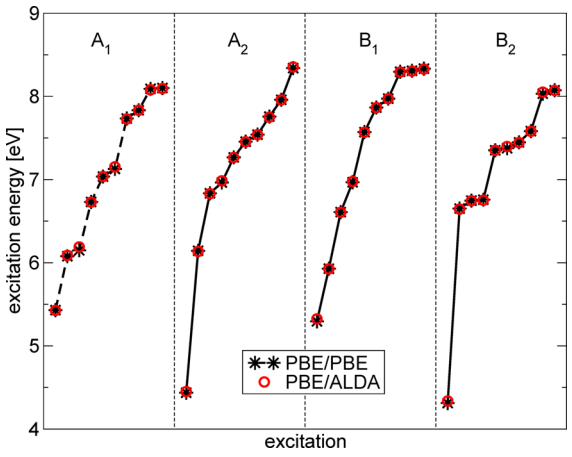

Figure 3. Pyridine molecule: comparison between TDDFT excitation energies employing the PBE xc potential and the PBE and ALDA xc kernel, respectively.

pyridine molecule calculated with the PBE functional but using two different local xc kernels, the adiabatic PBE xc kernel (the exact functional derivative of the PBE xc potential) and the ALDA xc kernel. As one can see in the figure, the excitation energies from both approaches are practically identical. In turn, this means that TDDFT calculations employing adiabatic local (LDA or GGA) xc kernels may yield different results for excitation energies solely due to differences of the xc potential. A comparsion of the errors for the PBE0AC(BRJ)/ALDA method of this work (see Tables 2, 3, and 4) with the errors for the set of GGA functionals (Figure 2) shows that they are similar for the valence excitations for the azabenzene molecules but clearly different for the excitations of the alkene and carbonyl group of molecules where the GGA approximations used in the work of Caricato et al. exceed an average error 1.0 kcal/mol while for the PBE0AC(BRJ)/ALDA approach of this work the deviation to the experimental values is much smaller and amounts to 0.23 kcal/mol, see Tables 2 and 3. Clearly, this difference is related to the fact that none of the GGA xc potentials used in the work of Caricato et al. are asymptotically corrected and thus are unable to describe Rydberg excitations qualitatively correct. The bottom left diagram in Figure 2 shows that the strong errors for the GGA functionals are noticeably corrected by using hyper-GGA functionals, which again can be attributed to the corrections of the long-range behavior of the underlying xc potentials.

A comparison of the errors for the RPA, RPAX(0.2), and RPAXerfJ(0.2) approximations of this work to the reference values of Caricato et al. shows that already with the RPA method, excluding any exchange-correlation contributions in the Hessian matrix, the mean absolute error for all considered states (upper left diagram in Figure 2) are smaller than both, for the EOM-CCSD method and the best hyper-GGA functional used in the work of Caricato et al. This again clearly demonstrates the importance of the impact of the quality of the xc potential used in TDDFT methods. The best performing functional of ref 31 is the B3P86 functional, which has a mean absolute error of 0.38 eV for all states (see top right diagram in Figure 2). It yields, however, an unbalanced description for the alkene+carbonyl and azabenzene groups: in the former case, the average error amounts to 0.47 eV, while in the latter case it amounts to 0.21 eV. This again is a consequence of the poor description of Rydberg excited states with standard (hybrid-)GGA functionals.

Noticeable improvements over the RPA results, as discussed in section 4.1, are obtained by the RPAXerfJ(0.2) approximation, which yields the smallest errors for all considered groups of excitations displayed in Figure 2, primarily for the valence excitations of the azabenzene molecules where the xc kernel has a larger impact (see discussion in section 4.1), see bottom right diagram of the figure.

4.3. Performance for Long-Range Excitations. Table 5 shows local (L) and charge-transfer (CT) excitation energies for the *N*-phenylpyrrole (PP) molecule and three model polypeptides from ref 35 for the RPAX(0.2) and RPAXerfJ(0.2) methods (employing the PBE0AC(BRJ) xc potential for the ground-state KS calculations). The results are compared with three different TDDFT methods used in ref 35: PBE (standard GGA functional), B3LYP (hybrid-GGA with 20% exact exchange), and CAM-B3LYP (range-separated GGA functional with 65% long-range exact exchange). Accurate CASPT2 and CCSD reference values for the considered excitations are compiled in the last column of the table and are taken from refs 93 and 94.

As can be seen in Table 5, all TDDFT methods describe the local excitations for the considered molecules quite well. The only significant exception for this is observed for PP/A_1 where the PBE and RPAX(0.2) methods underestimate the CCSD reference excitation energy by about 0.4 eV and for β-dipeptide/$n_2 \rightarrow \pi_2^*$ where all TDDFT methods overestimate the CASPT2 reference excitation energy by 0.3−0.7 eV. In section 4.2, it has been shown that, if local excitations are considered and when the experimental excitation energies are used as a reference, accurate TDDFT methods (employing accurate xc potentials) can compete with configuration-interaction or coupled-cluster wave function methods regarding

DOI: 10.1021/acs.jctc.5b00024
J. Chem. Theory Comput. XXXX, XXX, XXX−XXX

Table 5. Local (L) and Charge-Transfer (CT) Excitation Energies of *N*-Phenylpyrrole (PP) and Three Polypeptide Molecules (in eV)

molecule	excitation		PBE[a]	B3LYP[a]	CAM-B3LYP[a]	RPAX α = 0.2	RPAXerfJ α,β = 0.2	ref.[b,c]
PP	B_2	L	4.33	4.76	5.06	4.30	4.54	4.77
	A_1	L	4.61	4.96	5.12	4.69	4.87	4.98
	B_2	CT	3.98	4.58	5.27	4.17	4.99	5.40
	A_1	CT	3.90	4.64	5.92	4.08	5.47	6.06
dipeptide	$n_1\rightarrow\pi_2^*$	CT	4.61	6.31	7.84	5.29	6.92	8.07
	$\pi_1\rightarrow\pi_2^*$	CT	5.16	6.15	7.00	5.56	6.35	7.18
	$n_1\rightarrow\pi_1^*$	L	5.35	5.55	5.68	5.70	5.60	5.62
	$n_2\rightarrow\pi_2^*$	L	5.67	5.77	5.92	5.91	5.72	5.79
β-dipeptide	$n_1\rightarrow\pi_2^*$	CT	4.78	7.26	8.38	5.80	7.54	9.13
	$\pi_1\rightarrow\pi_2^*$	CT	5.32	7.20	8.01	5.72	7.05	7.99
	$n_1\rightarrow\pi_1^*$	L	5.38	5.66	5.67	5.42	5.53	5.40
	$n_2\rightarrow\pi_2^*$	L	5.41	5.56	5.76	5.52	5.58	5.10
tripeptide	$\pi_1\rightarrow\pi_2^*$	CT	5.18	6.27	6.98	5.55	6.38	7.01
	$\pi_2\rightarrow\pi_3^*$	CT	5.51	6.60	7.69	6.09	6.63	7.39
	$\pi_1\rightarrow\pi_3^*$	CT	4.76	6.06	8.51	5.72	8.24	8.74
	$n_1\rightarrow\pi_3^*$	CT	4.26	6.12	8.67	5.54	8.33	9.30
	$n_2\rightarrow\pi_3^*$	CT	5.16	6.83	8.25	6.13	7.41	8.33
	$n_1\rightarrow\pi_2^*$	CT	4.61	6.33	7.78	5.28	6.91	8.12
	$n_1\rightarrow\pi_1^*$	L	5.36	5.57	5.72	5.67	5.59	5.74
	$n_2\rightarrow\pi_2^*$	L	5.58	5.74	5.93	5.99	5.74	5.61
	$n_3\rightarrow\pi_3^*$	L	5.74	5.88	6.00	5.82	5.80	5.91

[a]TDDFT reference values taken from ref 35. [b]CASPT2 reference values for the polypeptide molecules from ref 94. [c]CCSD reference values for the PP molecule from ref 93.

the accuracy, so that one cannot rule out here that the wave function reference values in Table 5 are less accurate than the DFT values for the local excitations.

Considering the CT excitations in Table 5, however, it can be seen that there exist large differences between the different TDDFT approaches. As expected, in case of the PBE and RPAX(0.2) methods the CT excitations are strongly underestimated by a magnitude of 1−4 eV. A comparison of the results of these two methods shows, however, that especially for the $n \rightarrow \pi^*$ excitations of the polypeptides the RPAX(0.2) CT excitations are larger in magnitude than the PBE ones and thus have smaller deviations to the reference values of Table 5. A further improvement for the CT excitations is obtained with the B3LYP method with errors of about 10−30%. The respective largest errors of B3LYP of 31 and 34% are found for the far-range $n_1 \rightarrow \pi_3^*$ and $\pi_1 \rightarrow \pi_3^*$ excitations of the tripeptide molecule, which shows that there is a relation between the range of the excitation and the accuracy with which it can be described by hybrid-TDDFT methods.

Significant improvements over the B3LYP method for all CT transitions displayed in Table 5 are observed with the RPAXerfJ(0.2) method. With this approach the relative deviation to the reference values for all 10 CT excitation energies lie in the range of 6−15%. It is also apparent that the errors of the RPAXerfJ(0.2) for the far-range CT excitations is not larger than for the more short-range ones. On the contrary, for the tripeptide/$n_1 \rightarrow \pi_3^*$ excitation, the percentual deviation to the CASPT2 result is only 5.7%, which indicates that the performance of the method for CT excitations improves when the donor and acceptor states have a larger distance from each other. It can be assumed that this is related to the form of the erf-range function (eq 19) of the RPAXerfJ(0.2) method as it regulates how strong donor−acceptor orbital terms contribute to the Hessian matrix.

The best performance among the considered TDDFT methods for the CT states of Table 5 is found for the CAM-B3LYP method with an average percentual error of 3.1% only. This shows that current range-separated TDDFT methods can describe long-range excitations quite accurately, see also refs 33−37. While the RPAXerfJ(0.2) method of this work gives generally less accurate CT excitation energies, from the results of Table 5 it can be expected that it commonly outperforms standard hybrid functionals (with 20−30% of exact exchange) in this case.

5. SUMMARY

Molecular excitation energies have been calculated with time-dependent density functional theory (TDDFT) methods employing asymptotically corrected exchange-correlation (xc) potentials and random-phase approximation (RPA) Hessians augmented by exchange interactions. The xc potentials used in this work were two asymptotically corrected and localized approximations to the PBE0 xc potential and were shown to provide very accurate Rydberg excitations for a number of alkene and carbonyl molecules. In the case of valence excitations, where the xc kernel gives a stronger contribution to the Hessian matrix, it has been observed that different particle−hole exchange interaction contributions (RPAX(α) approaches) did not significantly improve the RPA results. These, however, were found to be as accurate as obtained with a number of hyper-GGA TDDFT methods (including also range-separated functionals) considered in the work by Caricato et al.[31] when compared to experimental reference excitation energies, provided again that accurate xc potentials

DOI: 10.1021/acs.jctc.5b00024
J. Chem. Theory Comput. XXXX, XXX, XXX−XXX

are used in the ground-state calculations. Significant improvements for local excitation energies could be obtained by including long-range particle−particle and hole−hole interactions. The resulting approach, termed as RPAXerfJ in this work, yields errors of about 0.14 eV on average only for the lowest excitations of a set of 11 molecules (66 excitations altogether) from the benchmark set of Caricato et al.[31] With this, the RPAXerfJ outperforms all wave function (including CIS(D) and EOM-CCSD) and TDDFT methods used in the study of Caricato et al.[31] for the examined set of transitions.

Long-range charge-transfer (CT) excitations were studied for a set of four molecules taken from a work by Peach et al.[35] While, as expected, the RPAX(α = 0.2) method strongly underestimates CT excitations by about 19% on average, it has been found that it typically improves standard generalized-gradient (GGA) TDDFT methods for which an average error of 23% is observed.[35] The RPAXerfJ($\alpha = \beta$ = 0.2) approach, including long-range donor−acceptor Coulomb interactions, again improves upon the RPAX(0.2) method and underestimates CT excitations by only 8% on average. This is clearly better than with standard hybrid functionals including 20% of exact exchange (B3LYP, error of 13%) but still larger than with common range-separated functionals (CAM-B3LYP, error of 3%). A comparison of the errors for the shorter range and longer range CT excitations for the RPAXerfJ(0.2) indicates, however, that the error becomes smaller in the case of longer range excitations. This might be related to the fact that donor−acceptor Coulomb interactions are not damped anymore by the erf-Coulomb interaction when the distance between donor and acceptor orbital exceeds the damping range of the error function. In order to achieve a higher accuracy also for more short-range CT excitations with the RPAXerfJ method, larger values for the range-parameter β have to be used, counteracting, however, the accuracy for local valence excitations. This has been tested for the dipeptide molecule by increasing the value of β to 0.4. As a result, the CT transitions increased by values of 0.76 eV in the case of the $\pi_1 \rightarrow \pi_2^*$ excitation and even 1.61 eV in the case of the $n_1 \rightarrow \pi_2^*$ excitation, thus strongly improving the original values, see Table 5. At the same time, however, this lead to a downward shift of the two local excitations of about 0.33 eV in each case, deteriorating the results of the RPAXerfJ($\alpha = \beta$ = 0.2) approach. To achieve a more balanced accuracy for local and CT excitations, therefore, a modification of the proposed approximations for the Hessian seems to be necessary. This has to be analyzed in future works.

AUTHOR INFORMATION

Corresponding Author

*E-mail: andreas.hesselmann@chemie.uni-erlangen.de.

Notes

The authors declare no competing financial interest.

REFERENCES

(1) *Time-Dependent Density Functional Theory: Lecture Notes in Physics*; Marques, M. A. L., Ed.; Springer: Heidelberg, 2006; Vol. *706*.
(2) Gross, E. K. U.; Dobson, J. F.; Petersilka, M. *Springer Series in Topics in Current Chemistry (Density Functional Theory II)*; Nalewajski, R. F., Ed.; Springer: Heidelberg, 1996; Vol. *181*, p 81.
(3) Laurent, A. D.; Jacquemin, D. *Int. J. Quantum Chem.* **2013**, *113*, 2019.
(4) Casida, M. E. *J. Mol. Struct. (THEOCHEM)* **2009**, *914*, 3.
(5) Elliot, P.; Furche, F.; Burke, K. *Rev. Comp. Chem.* **2009**, *26*, 91.
(6) Casida, M. E.; Huix-Rotllant, M. *Annu. Rev. Phys. Chem.* **2012**, *63*, 287.
(7) Runge, E.; Gross, E. K. U. *Phys. Rev. Lett.* **1984**, *52*, 997.
(8) Hohenberg, P.; Kohn, W. *Phys. Rev. A* **1964**, *136*, B864.
(9) Görling, A. *Phys. Rev. A* **1992**, *46*, 3753.
(10) Wang, Y.; Parr, R. G. *Phys. Rev. A* **1993**, *47*, R1591.
(11) Zhao, Q.; Morrison, R. C.; Parr, R. G. *Phys. Rev. A* **1994**, *50*, 2138.
(12) van Leeuwen, R.; Baerends, E. J. *Phys. Rev. A* **1994**, *49*, 2421.
(13) Gritsenko, O. V.; van Leeuwen, R.; Baerends, E. J. *Phys. Rev. A* **1995**, *52*, 1870.
(14) Görling, A.; Ernzerhof, M. *Phys. Rev. A* **1995**, *51*, 4501.
(15) Tozer, D. J.; Ingamells, V. E.; Handy, N. C. *J. Chem. Phys.* **1996**, *105*, 9200.
(16) Wu, Q.; Yang, W. *J. Chem. Phys.* **2003**, *118*, 2498.
(17) Kadantsev, E. S.; Stott, M. J. *Rhys. Rev. A* **2004**, *69*, 012502.
(18) Astala, R.; Stott, M. J. *Phys. Rev. B* **2006**, *73*, 115127.
(19) van Gisbergen, S. J. A.; Kootstra, F.; Schipper, P. R. T.; Gritsenko, O.; Snijders, J. G.; Baerends, E. J. *Phys. Rev. A* **1998**, *57*, 2556.
(20) Görling, A. *Int. J. Quantum Chem.* **1998**, *69*, 265.
(21) Görling, A. *Phys. Rev. A* **1998**, *57*, 3433.
(22) Gritsenko, O. V.; Baerends, E. J. *Phys. Rev. A* **2001**, *64*, 042506.
(23) Gritsenko, O.; Baerends, E. J. *J. Chem. Phys.* **2004**, *121*, 655.
(24) Maitra, N. T. *J. Chem. Phys.* **2005**, *122*, 234104.
(25) Maitra, N. T.; Tempel, D. G. *J. Chem. Phys.* **2006**, *125*, 184111.
(26) Bokhan, D.; Bartlett, R. J. *Phys. Rev. A* **2006**, *73*, 022502.
(27) Gritsenko, O. V.; Baerends, E. J. *Phys. Chem. Chem. Phys.* **2009**, *11*, 4640.
(28) Heßelmann, A.; Ipatov, A.; Görling, A. *Phys. Rev. A* **2009**, *80*, 012507.
(29) Ipatov, A.; Heßelmann, A.; Görling, A. *Int. J. Quantum Chem.* **2010**, *110*, 2202.
(30) Parr, R. G., Yang, W. *Density-Functional Theory of Atoms and Molecules*; Oxford University Press: Oxford, 1989.
(31) Caricato, M.; Trucks, G. W.; Frisch, M. J.; Wiberg, K. B. *J. Chem. Theory Comput.* **2010**, *6*, 370.
(32) Jacquemin, D.; Wathelet, V.; Perpete, E. A.; Adamo, C. *J. Chem. Theory Comput.* **2009**, *5*, 2420.
(33) Yanai, T.; Tew, D. P.; Handy, N. C. *Phys. Rev. Lett.* **2004**, *393*, 51.
(34) Peach, M. J. G.; Helgaker, T.; Salek, P.; Keal, T. W.; Lutnaes, O. B.; Tozer, D. J.; Handy, N. C. *Phys. Chem. Chem. Phys.* **2006**, *8*, 558.
(35) Peach, M. J. G.; Benfield, P.; Helgaker, T.; Tozer, D. J. *J. Chem. Phys.* **2008**, *128*, 044118.
(36) Akinaga, Y.; Ten-No, S. *Int. J. Quantum Chem.* **2009**, *109*, 1905.
(37) Kuritz, N.; Stein, T.; Baer, R.; Kronik, L. *J. Chem. Theory Comput.* **2011**, *7*, 2408.
(38) Dreuw, A.; Plötner, J.; Wormit, M.; Head-Gordon, M.; Dutoi, A. D. *Z. Phys. Chem.* **2010**, *224*, 311.
(39) Lembarki, A.; Rogemond, F.; Chermette, H. *Phys. Rev. A* **1995**, *52*, 3704.
(40) Gritsenko, O. V.; van Leeuwen, R.; Baerends, E. J. *Int. J. Quantum Chem.* **1997**, *61*, 231.
(41) Karasiev, V.; Ludena, E. V.; Lopez-Boada, R. *Int. J. Quantum Chem.* **1998**, *70*, 591.
(42) Gritsenko, O. V.; Schipper, P. R. T.; Baerends, E. J. *Chem. Phys. Lett.* **1999**, *302*, 199.
(43) Gritsenko, O. V.; Schipper, P. R. T.; Baerends, E. J. *Int. J. Quantum Chem.* **2000**, *76*, 407.
(44) Schipper, P. R. T.; Gritsenko, O. V.; van Gisbergen, S. J. A.; Baerends, E. J. *J. Chem. Phys.* **2000**, *112*, 1344.
(45) Karasiev, V.; Ludena, E. V. *Phys. Rev. A* **2002**, *65*, 032515.
(46) Becke, A. D.; Johnson, E. R. *J. Chem. Phys.* **2006**, *124*, 221101.
(47) Gaiduk, A. P.; Staroverov, V. N. *J. Chem. Phys.* **2012**, *136*, 064116.
(48) Tozer, D. J.; Handy, N. C. *J. Chem. Phys.* **1998**, *109*, 10180.
(49) Casida, M. E.; Salahub, D. R. *J. Chem. Phys.* **2000**, *113*, 8918.
(50) Allen, M. J.; Tozer, D. J. *J. Chem. Phys.* **2000**, *113*, 5185.

DOI: 10.1021/acs.jctc.5b00024
J. Chem. Theory Comput. XXXX, XXX, XXX−XXX

(51) Grüning, M.; Gritsenko, O. V.; van Gisbergen, S. J. A.; Baerends, E. J. *J. Chem. Phys.* **2001**, *114*, 652.
(52) Grüning, M.; Gritsenko, O. V.; van Gisbergen, S. J. A.; Baerends, E. J. *J. Chem. Phys.* **2002**, *116*, 9591.
(53) Hirata, S.; Zhan, C.-G.; Apra, E.; Windus, T. L.; Dixon, D. A. *J. Phys. Chem. A* **2003**, *107*, 10154.
(54) Wu, Q.; Ayers, P. W.; Yang, W. *J. Chem. Phys.* **2003**, *119*, 2978.
(55) Hirata, S.; Ivanov, S.; Grabowski, I.; Bartlett, R. J. *J. Chem. Phys.* **2002**, *116*, 6468.
(56) Shigeta, Y.; Hirao, K.; Hirata, S. *Phys. Rev. A* **2006**, *73*, 010502.
(57) Hellgreen, M.; von Barth, U. *J. Chem. Phys.* **2009**, *131*, 044110.
(58) Heßelmann, A.; Görling, A. *J. Chem. Phys.* **2011**, *134*, 034120.
(59) Grüneis, A.; Marsman, M.; Harl, J.; Schimka, L.; Kresse, G. *J. Chem. Phys.* **2009**, *131*, 154115.
(60) Heßelmann, A. *Phys. Rev. A* **2012**, *85*, 012517.
(61) Bates, J. E.; Furche, F. *J. Chem. Phys.* **2013**, *139*, 171103.
(62) Heßelmann, A. *Springer Series in Topics in Current Chemistry (Density Functionals: Thermochemistry)*; Springer: Heidelberg, 2014; Chapter: The ring and exchange-ring approximations based on Kohn−Sham reference states.
(63) Heßelmann, A.; Görling, A. *Mol. Phys.* **2010**, *108*, 359.
(64) Heßelmann, A.; Görling, A. *Phys. Rev. Lett.* **2011**, *106*, 093001.
(65) Heßelmann, A.; Görling, A. *Mol. Phys.* **2011**, *109*, 2473.
(66) Perdew, J. P.; Burke, K.; Ernzerhof, M. *Phys. Rev. Lett.* **1996**, *77*, 3865.
(67) Adamo, C.; Barone, V. *Chem. Phys. Lett.* **1997**, *274*, 242.
(68) Adamo, C.; Barone, V. *J. Chem. Phys.* **1999**, *110*, 6158.
(69) Harris, F. E.; Monkhorst, H. J.; Freeman, D. L. *Algebraic and diagrammatic methods in many-fermion theory*; Oxford University Press: 1992; p 56f.
(70) (a) Chong, D. P.; Gritsenko, O. V.; Barends, E. J. *J. Chem. Phys.* **2002**, *116*, 1760. (b) van Meer, R.; Gritsenko, O. V.; Barends, E. J. *Chem. Theory Comput.* **2014**, *10*, 4432.
(71) Sharp, R. T.; Horton, G. K. *Phys. Rev.* **1953**, *90*, 317.
(72) Talman, J. D.; Shadwick, W. F. *Phys. Rev. A* **1976**, *14*, 36.
(73) Holas, A.; Cinal, M. *Phys. Rev. A* **2005**, *72*, 032504.
(74) Becke, A. D.; Roussel, M. R. *Phys. Rev. A* **1989**, *39*, 3761.
(75) Ivanov, S.; Hirata, S.; Bartlett, R. *J. Phys. Rev. Lett.* **1999**, *83*, 5455.
(76) Kümmel, S.; Perdew, J. P. *Phys. Rev. Lett.* **2003**, *90*, 043004.
(77) Wu, Q.; Yang, W. *J. Theor. Comp. Chem.* **2003**, *2*, 627.
(78) Heßelmann, A.; Götz, A. W.; della Sala, F.; Görling, A. *J. Chem. Phys.* **2007**, *127*, 054102.
(79) Neumann, R.; Nobes, R. H.; Handy, N. C. *Mol. Phys.* **1996**, *87*, 1.
(80) Heßelmann, A.; Manby, F. *J. Chem. Phys.* **2005**, *123*, 164116.
(81) Gritsenko, O.; van Leeuwen, R.; Baerends, E. J. *Int. J. Quantum Chem.* **1996**, *57*, 17.
(82) van Leeuwen, R.; Gritsenko, O. V.; Baerends, E. J. *Topics in Current Chemistry*; Springer-Verlag: Berlin, 1996; Vol. *180*, Chapter Analysis and Modelling of Atomic and Molecular Kohn-Sham Potential, p 107.
(83) Della Sala, F.; Görling, A. *J. Chem. Phys.* **2001**, *115*, 5718.
(84) Görling, A.; Ipatov, A.; Götz, A. W.; Heßelmann, A. *Z. Phys. Chem.* **2010**, *224*, 325.
(85) Görling, A.; Heßelmann, A.; Jones, M.; Levy, M. *J. Chem. Phys.* **2008**, *128*, 104104.
(86) Oddershede, J.; Jørgensen, P.; Yeager, D. L. *Comp. Phys. Rep.* **1984**, *2*, 33.
(87) Weiss, H.; Ahlrichs, R.; Häser, M. *J. Chem. Phys.* **1993**, *99*, 1262.
(88) Walker, I. C.; Palmer, M. H.; Hopkirk, A. *Chem. Phys.* **1990**, *141*, 365.
(89) Szabo, A.; Ostlund, N. S. *Modern Qantum Chemistry*; Dover Press: 1996.
(90) Toulouse, J.; Colonna, F.; Savin, A. *Phys. Rev. A* **2004**, *70*, 062505.
(91) Casida, M. E. *Recent Advances in Density Functional Methods*; Chong, D. P., Ed.; World Scientific: Singapore, 1995; Vol. *I*, p 155.
(92) Del Bene, J. E.; Watts, J. D.; Bartlett, R. J. *J. Chem. Phys.* **1997**, *106*, 6051.
(93) Peach, M. J. G.; Tozer, D. J. *J. Phys. Chem. A* **2012**, 9783.
(94) Serrano-Andres, L.; Fulscher, M. *J. Am. Chem. Soc.* **1998**, *120*, 10912.
(95) Dunning, T. H. *J. Chem. Phys.* **1989**, *90*, 1007.
(96) Kendall, R. A.; Dunning, T. H., Jr.; Harrison, R. J. *J. Chem. Phys.* **1992**, *96*, 6796−6806.
(97) Woon, D.; Dunning, T. H., Jr. *J. Chem. Phys.* **1994**, *100*, 2975.
(98) Weigend, F.; Köhn, A.; Hättig, C. *J. Chem. Phys.* **2002**, *116*, 3175.
(99) Werner, H.-J.; Knowles, P. J.; Knizia, G.; Manby, F. R.; Schütz, M.; Celani, P.; Korona, T.; Lindh, R.; Mitrushenkov, A.; Rauhut, G.; Shamasundar, K. R.; Adler, T. B.; Amos, R. D.; Bernhardsson, A.; Berning, A.; Cooper, D. L.; Deegan, M. J. O.; Dobbyn, A. J.; Eckert, F.; Goll, E.; Hampel, C.; Hesselmann, A.; Hetzer, G.; Hrenar, T.; Jansen, G.; Köppl, C.; Liu, Y.; Lloyd, A. W.; Mata, R. A.; May, A. J.; McNicholas, S. J.; Meyer, W.; Mura, M. E.; Nicklass, A.; O'Neill, D. P.; Palmieri, P.; Peng, D.; Pflüger, K.; Pitzer, R.; Reiher, M.; Shiozaki, T.; Stoll, H.; Stone, A. J.; Tarroni, R.; Thorsteinsson, T.; Wang, M. *MOLPRO*, version 2012.1. See http://www.molpro.net.
(100) Werner, H.-J.; Knowles, P. J.; Knizia, G.; Manby, F. R.; Schütz, M. *WIREs Comput. Mol. Sci.* **2012**, *2*, 242−253.
(101) Ahlrichs, R.; Bär, M.; Häser, M.; Horn, H.; Kölmel, C. *Chem. Phys. Lett.* **1989**, *162*, 165.
(102) Wiberg, K. B.; de Olivera, A. E.; Trucks, G. *J. Phys. Chem. A* **2002**, *106*, 4192.
(103) Wiberg, K. B.; Hadad, C. M.; Ellison, G. B.; Foresman, J. B. *J. Phys. Chem.* **1993**, *97*, 13586.
(104) Hadad, C. M.; Foresman, J. B.; Wiberg, K. B. *J. Phys. Chem.* **1993**, *97*, 4293.
(105) Bolovinos, A.; Tsekeris, P.; Philis, J.; Pantos, E.; Andritsopolous, G. J. *J. Mol. Spectrosc.* **1984**, *103*, 240.
(106) Goodman, L. J. *J. Mol. Spectrosc.* **1961**, *6*, 109.
(107) Innes, K. K.; Ross, I. G.; Moomaw, W. R. *J. Mol. Spectrosc.* **1988**, *132*, 492.
(108) Palmer, M. H.; Walker, I. C. *Chem. Phys.* **1991**, *157*, 187.
(109) Palmer, M. H.; McNab, H.; Reed, D.; Pollacchi, A.; Walker, I. C.; Guest, M. F.; Siggel, M. R. F. *Chem. Phys.* **1997**, *214*, 191.
(110) Spencer, G. H.; Cross, P. C.; Wiberg, K. B. *J. Chem. Phys.* **1961**, *35*, 1925.
(111) Adamo, C.; Barone, V. *Chem. Phys. Lett.* **2000**, *330*, 152.
(112) Nooijen, M. *J. Phys. Chem. A* **2000**, *104*, 4553.
(113) Devarajan, A.; Gaenko, A. V.; Khait, Y. G.; Hoffmann, M. R. *J. Phys. Chem. A* **2008**, *112*, 2677.

DOI: 10.1021/acs.jctc.5b00024
J. Chem. Theory Comput. XXXX, XXX, XXX−XXX